Published in final edited form as:
Mol Cancer Res. 2013 November ; 11(11): . doi:10.1158/1541-7786.MCR-13-0108.

Inhibition of Cell Adhesion by an Anti-cadherin 11 Antibody Prevents Bone Metastasis

Yu-Chen Lee[#1], **Mehmet Asim Bilen**[#1], **Guoyu Yu**[#1], **Song-Chang Lin**[1], **Chih-Fen Huang**[1,3], **Angelica Ortiz**[1], **Hyojin Cho**[1], **Jian H. Song**[1], **Robert L. Satcher**[1], **Jian Kuang**[1], **Gary E. Gallick**[1], **Li-Yuan Yu-Lee**[2], **Wilber Huang**[4], and **Sue-Hwa Lin**[1]

[1]Departments of Translational Molecular Pathology, Genitourinary Medical Oncology, Orthopaedic Oncology, Experimental Therapeutics, The University of Texas M. D. Anderson Cancer Center, Houston, Texas

[2]Department of Medicine, Baylor College of Medicine, Houston, Texas

[3]Department of Pharmacy at National Taiwan University Hospital, Taipei, Taiwan

[4]Abnova Corporation, Taiwan

[#] These authors contributed equally to this work.

Abstract

Cadherin-11 is a member of a superfamily mainly expressed in osteoblasts but not in epithelial cells. However, prostate cancer (PCa) cells with bone metastasis propensity express high levels of cadherin-11 and reduced levels of E-cadherin. Downregulation of cadherin-11 inhibits interaction of PCa cells with osteoblasts in vitro and homing of PCa cells to bone in an animal model of metastasis. These findings raise the possibility that targeting the extracellular domain of cadhein-11 may prevent PCa bone metastasis. To explore this possibility, we generated a panel of monoclonal antibodies (mAbs) against cadherin-11 extracellular domain. From the 21 antibodies obtained, mAbs 2C7 and 1A5 inhibited cadherin-11 mediated cell-cell aggregation in L-cells transfected with cadherin-11 in vitro. Both antibodies were specific to cadherin-11 as they did not recognize E-cadherin or N-cadherin on C4-2B or PC3 cells, respectively. Further, mAb 2C7 inhibited cadherin-11-mediated aggregation between PC3-mm2 cells and MC3T3-E1 osteoblasts. To determine which cadherin domains are critical for PCa and osteoblast interactions, a series of deletion mutants were analyzed. We identified a previously unknown unique motif, aa 343-348, in the cadherin-11 EC3 domain that is recognized by mAb 2C7 and showed that this motif mediated cell-cell adhesion. Consistent with the inhibition of cell-cell aggregation in vitro, application of mAb 2C7 in a prophylactic setting as a single agent effectively prevented dissemination of highly metastatic PC3-mm2 cells to bone in a mouse model of metastasis. These results suggest that targeting the extracellular domain of cadherin-11 may be developed for the prevention of bone metastases.

Keywords

cadherin-11; prostate cancer; adhesion; bone metastasis; osteoblast

To whom correspondence should be addressed: Sue-Hwa Lin, Ph.D. Department of Translational Molecular Pathology, The University of Texas M. D. Anderson Cancer Center, 1515 Holcombe Boulevard, Houston, TX, 77030, USA. Telephone 713-794-1559; Fax: 713-834-6084; slin@mdanderson.org.

CONFLICT OF INTEREST

The authors declare no conflict of interest.

Introduction

Advanced prostate cancer (PCa) often metastasizes to distant organ sites with bone being the most commonly affected site (1). One of the contributors to the lethal progression of the disease is the abnormal expression of cadherin-11 (Cad11) in prostate cancer cells (2). Cad11 is the physiological cadherin molecule expressed on osteoblasts (3). However, our previous studies demonstrated that PCa cells, especially those in bone metastases, often switch the cadherin type from E-cadherin to Cad11, due to epithelial-mesenchymal transition (EMT) (2). This EMT transition enables PCa cells to interact with osteoblasts in bone (4). Moreover, downregulation of Cad11 in highly metastatic PC3-mm2 cells with Cad11-specific short hairpin RNA significantly decreased the incidence of PC3-mm2 metastasis to bone in an animal model of metastasis (2). These findings suggest that targeting Cad11-mediated cell-cell interaction may be a promising strategy in preventing PCa bone metastasis.

Inhibition of Cad11-mediated PCa and osteoblast interaction can be achieved through small molecules or antibodies that recognize the extracellular domain of Cad11. Because PCa is often detected early and there is nearly a 10-year “window” during which anti-metastasis therapy would be useful as “secondary prevention”, the stability and efficacy of the targeting agents will be key factors for the feasibility and success of the treatment. As compared to small molecules, antibodies are more stable in the circulation and thus more suitable for chronic administration in a prophylactic setting for the prevention of metastases in patients with a high risk of developing bone metastasis. The objective of this study is to determine the feasibility of developing an antibody-based prevention strategy that targets Cad11.

Three tasks need to be fulfilled in the early stages of developing antibodies that target Cad11-mediated cell-cell adhesion. The first task is to develop an antibody that has the desired activities for performing proof-of-concept studies. The second task is to test the concept that targeting the extracellular domain of Cad11 is able to prevent PCa metastasis in an animal model system in vivo. Although our previous studies demonstrated that Cad11 knockdown inhibits PCa metastasis in an animal model of metastasis, it was not clear whether the inhibition of extracellular interactions is sufficient to inhibit metastasis to bone. The third task is to identify the region/motif in the extracellular domain of Cad11 that can be recognized by the antibodies. Identification of this motif will lay the foundation for developing more effective antibodies that target Cad11 mediated cell-cell interaction for clinical application.

In this study, we generated 21 antibodies against the extracellular domain of Cad11 and identified two promising candidates from this panel. We identified a previously unknown adhesion motif in the extracellular domain of Cad11 that is recognized by both antibodies. We further performed animal studies with one of the characterized antibodies and obtained evidence that targeting this unique motif in the third extracellular domain (EC3) of Cad11 by the antibody is effective in reducing PCa metastasis to bone.

Experimental Procedures

Materials

C4-2B4-Cad11 expressing Cad11 and GFP, and PC3-mm2-Luc expressing luciferase and GFP, were generated as described previously (2, 4). PC3-mm2 and C4-2B4 cell lines were confirmed by fingerprinting. Goat anti-Cad11 polyclonal antibody was purchased from R&D Systems.

Cell aggregation assay

L-cells (CCL1.3) expressing Cad11 (L-Cad11) were generated by infecting L-cells with recombinant retroviruses expressing Cad11 and GFP as previously described (5). Control L-vector cells express only GFP. L-cells or L-Cad11 cells were released from culture plates using Cellstripper (Cellgro, Mediatech, Inc., Manassas, VA) for 10-12 min at 37°C, suspended in DMEM medium plus 10% FBS, mixed on the rocker, and counted using a hemacytometer. Cell clusters containing 3 or more cells were considered as aggregates. PC3-mm2 cells and MC3T3-E1 osteoblasts were labeled with fluorescent dyes DiO and DiI, respectively. Labeled cells were trypsinized in the presence of 10 mM $CaCl_2$ and resuspended in medium containing 1% BSA, 100 units/ml DNase, with or without 1 mM $CaCl_2$, and 20 μg/ml IgG or mAb 2C7. Cell aggregation was analyzed as described above. Cell-to-substrate assay was performed as described previously (5).

Expression and purification of Cad11-Fc, Cad11-his$_7$ recombinant proteins and generation of anti-Cad11 monoclonal antibodies

Cad11-Fc protein, containing the extracellular domain of Cad11 fused to Fc, was prepared as described (5). Cad11-his$_7$ protein, containing the extracellular domain of Cad11 with a 7-histidine tag in the C-terminus, was constructed as follows. The pBMN-(OB-CAD-Fc)-I-GFP plasmid (5), which was used to generate OB-Fc, was digested with BamHI and NotI to remove the DNA fragment encoding the Fc protein. The pBMN-(OB-CAD-Fc)-I-GFP without the Fc fragment was then ligated with oligonucleotides (Supplemental Table S1) encoding 7 histidine residues, a termination codon, and BamHI and NotI restriction sites at its 5′ and 3′ ends, respectively. The resulting plasmid, pBMN-(Cad11-his$_7$)-I-GFP, was used to generate retrovirus and transduce 293FT cell line as described previously (5). To purify Cad11-his protein, 293FT cells expressing Cad11-his$_7$ were grown on 10-cm plates in DMEM supplemented with 10% FBS until 80–90% confluency. The serum-containing medium was collected after two days and concentrated 10 times in an Amicon Ultra-15 Centrifugal Filter (Millipore, Billerica, MA). Cad11-his$_7$ fusion protein was purified by Ni-NTA agarose as described previously (6). Mice were immunized with Cad11-Fc protein and the monoclonal antibodies screened by ELISA assays using Cad11-his$_7$-coated plates.

Fluorescence activated cell sorting analysis

Fluorescence activated cell sorting analyses (FACS) were performed as described previously (4).

Intracardiac injection, bioluminescence imaging of mouse, and qPCR

The luciferase and GFP-expressing cells (PC3-mm2-Luc) (1×10^6 cells/mouse) were mixed with control IgG (30 μg/mouse) or mAb 2C7 (30 μg/mouse) for 30 min before injecting into the left ventricle of male SCID mice. Mice were injected with antibodies immediately prior to tumor cell inoculation. Tumor growth was monitored weekly for 3 weeks using bioluminescence imaging. Images were acquired and analyzed with an IVIS Imaging System (Xenogen, Alameda, CA). Femurs and tibias were collected at the conclusion of the study and DNA was prepared using Tissue and Blood DNA kit (Invitrogen, Carlsbad, CA). Quantitative PCR was performed using oligonucleotides specific for human Alu sequence (Supplemental Table 1).

Generation of Cad11 extracellular domains for mAb epitope mapping

The extracellular domain DNA fragments EC1, EC2, EC3, and EC4, corresponding to the 1-159, 1-268, 1-383, 1-486 amino acid residues, respectively, of human Cad11 were cloned by PCR, confirmed by sequencing, and subcloned into pGEX4T-1 for the production of GST-tagged Cad11 proteins. A similar procedure was used to prepare EC3 containing serial

deletions from its C-terminus. Full-length Cad11 with mutations at tryptophan residues 2 and/or 4 (W2W4) or mAb 2C7 epitope were generated by overlapping PCR. The nucleotide sequences of primers used for deletions and mutagenesis are listed in Supplemental Table 1.

Generation of L-cell lines stably expressing mutant Cad11

Cad11 cDNA with mutations of the 6 amino acids in mAb 2C7 epitope to alanine (Cad11-6A) or mutations of the tryptophans at positions 2 and 4 to alanine (Cad11-W2A) were generated by overlapping PCR (see Supplemental Table 1). The mutant Cad11 cDNAs were cloned into the retroviral vector pBMN-I-neo, generated by replacing GFP cDNA in pBMN-I-GFP with that for the neo gene. L-cells infected with retroviruses were selected in G418-containing media.

Statistical analyses

Two-tailed, paired Student's t test was used for the statistical analysis of the data. A P-value of less than 0.05 was considered statistically significant. Data are expressed as the means ± SD.

Results

Inhibition of Cad11-mediated cell aggregation by antibodies

To examine whether antibodies could be used to block Cad11-mediated adhesion, an affinity-purified anti-Cad11 polyclonal antibody generated against the extracellular domain of Cad11 was examined for its effect on Cad11-mediated cell aggregation. An L-cell based adhesion assay was established for identifying agents that inhibit cadherin-11-mediated cell-cell aggregation. L-cells are murine fibroblasts that do not adhere to one another as they do not express cell adhesion molecules. Thus, L-cells were transfected with control vector (L-vector) or Cad11 cDNA (L-Cad11). Cell aggregation was measured as a decrease in single cell numbers. As shown in Fig. 1A, expression of Cad11 led to cell aggregation, with a 70% decrease in single cell number after 3 hr. In contrast, the L-vector alone led to only an approximate 10% decrease in single cell number during the 3 hr assay (Fig. 1A).

At the concentration of 20 μg/ml, the polyclonal anti-Cad11 antibody exhibited a time- (Fig. 1B) and dose-dependent (Fig. 1C) inhibition of adhesion, while the control IgG did not affect the aggregation phenotype. Increasing the antibody concentration to 50 μg/ml did not result in further inhibition of cell aggregation (data not shown). In addition, the polyclonal anti-Cad11 antibody can achieve only a 50% maximal inhibition (Fig. 1C). It is possible that only a small fraction of the polyclonal antibody is able to block the aggregation. Nevertheless, these observations suggest that generation and selection for an antibody that blocks Cad11-mediated cell-cell aggregation may be used to determine the role of adhesion on bone metastasis.

Next, we generated Cad11-Fc and Cad11-his_7 that contain the extracellular domain of Cad11 fused with either Fc or 7-histidines. We used Cad11-Fc for immunization and Cad11-his_7 for antibody screening. Among a panel of 21 anti-Cad11 monoclonal antibodies (mAbs) generated, two mAbs 1A5 and 2C7 inhibited aggregation by more than 70% (Fig. 1D).

Characterization of anti-Cad11 mAb 2C7 and 1A5

Using L-Cad11 cells in FACS analysis, mAb 2C7 showed an approximate 2-fold increased binding to Cad11 compared to that of mAb 1A5 (Fig. 2A). Similarly, mAb 2C7 exhibited stronger signals compared to mAb 1A5 when detecting Cad11 in L-Cad11 cells by Western blot analyses (Fig. 2B). Thus, we focused subsequent analyses using mAb 2C7. Next, we examined the specificity of mAb 2C7 for cadherins expressed in PCa cells. C4-2B4 cells

express endogenous E-cadherin (Fig. 2C). By western blot analysis, mAb 2C7 does not cross-react with E-cadherin. In contrast, PC3 PCa cells and its subline, PC3-mm2 cells, express endogenous N-cadherin and Cad11. Anti-N-cadherin antibody reacted with proteins with molecular mass of 130 kDa while mAb 2C7 reacted with a protein of 100 kDa (Fig. 2C), suggesting that mAb 2C7 does not cross-react with N-cadherin. On FACS analysis, mAb 2C7 reacted with C4-2B4-Cad11 but not C4-2B4-vector cells (Fig. 2D). mAb 2C7 also strongly reacted with PC3-mm2 cells (Fig. 2D). Downregulation of Cad11 in PC3-mm2 cells by shRNA (PC3-mm2/shCad11) (4) significantly reduced mAb 2C7 binding to the cells (Fig. 2D). Similar results were observed with mAb 1A5 (data not shown). Together, these results suggest that mAb 2C7 and 1A5 specifically recognize endogenous Cad11 expressed in PC3 cells as well as exogenous Cad11 overexpressed in C4-2B4 cells.

mAb 2C7 inhibits adhesion between PC3-mm2 and MC3T3-E1 osteoblasts

Next, we examined whether inhibition of Cad11-mediated adhesion by mAb 2C7 is sufficient to block the interactions between PC3-mm2 cells and osteoblasts. We first determined the dose of mAb required for inhibiting Cad11-mediated adhesion. In L-Cad11 cells, mAb 2C7 at a concentration of 1 μg/ml was sufficient to detectably inhibit cell aggregation, and a 50% inhibition was reached at 2 μg/ml (Fig. 3A, left panel), in contrast to the polyclonal antibody, which exhibits a maximum inhibition of 50% at 20 μg/ml (Fig. 1E). The maximum inhibition (80%) was reached at a dose of 10 μg/ml as increasing the amount of antibody to 20 μg/ml did not further increase the inhibition (Fig. 3A, right panel). Mouse IgG, used as a control, had no effect on cell-cell aggregation. These observations suggest that mAb 2C7 inhibits the Cad11-mediated aggregation efficiently. We further examined the effects of mAb 2C7 on the aggregation between PC3-mm2, a metastatic PCa cell line that expresses endogenous Cad11, and MC3T3-E1, an immortalized osteoblast cell line. PC3-mm2 and MC3T3-E1 formed mixed aggregates in the presence of Ca^{2+} but not in Ca^{2+}-free medium (Fig. 3B). Addition of mAb 2C7 led to a significant inhibition of the Ca^{2+}-dependent PC3-mm2/MC3T3-E1 cell-cell aggregation (Fig. 3B).

mAb 2C7 does not inhibit Cad11-mediated migration and invasion

Our previous studies showed that expression of Cad11 also increases the migration and invasion, but not proliferation, of PCa cells (4). We thus examined whether mAb 2C7 and 1A5 can affect PCa cell migration or invasion. As shown in supplemental Figure S1, addition of mAbs 2C7 or 1A5 to C4-2B4/Cad11 cells did not affect cell migration or invasion. In contrast, mAb 1B9, which did not affect adhesion, was found to inhibit the migration (45%) and invasion (75%) of C4-2B4/Cad11 cells compared to those in controls (supplemental Figure S1A and B).

Identification of mAb 2C7 binding domain in Cad11

Next, we examined the mechanism by which mAb 2C7 inhibited Cad11-mediated cell-cell aggregation. Previous studies have shown that extracellular cadherin domain 1 (EC1) is responsible for the adhesive activity of cadherins, including E-, P-, and N-cadherin (7). Structural studies also showed that Tryptophan 2 and 4 located at the N-terminus of EC1 of Cad11 mediates self-association through interaction with hydrophobic amino acids within EC1 (8). However, using atomic force microscopy, domains other than EC1 have been reported to be involved in cadherin11-mediated adhesion (9-12). mAb 2C7 could inhibit Cad11-mediated adhesion either by binding to the known adhesion motif located at EC1 or through novel adhesion motif.

We first defined the domain to which mAb 2C7 epitope binds. We generated GST fusion proteins containing various lengths of Cad11 extracellular domain (Fig. 4A). Cad11 contains 5 extracellular cadherin repeats (ECs), each approximately 110 amino acids long (13). The

EC domain boundaries were derived from sequence alignment of the Cad11 amino acid sequence with that of other members of the cadherin family as described (13). Western blot showed that mAb 2C7 and 1A5 did not bind to either GST-EC1 or GST-EC2 but reacted with GST-EC3 (Fig. 4A), suggesting that both mAb 2C7 and mAb 1A5 epitopes are localized within the EC3 domain of Cad11.

We further refined the epitope within the EC3 domain. Five EC3 deletion mutants with sequential deletions of 20 amino acids from its C-terminus were generated. Western blot of mAb 2C7 or 1A5 with these mutants showed that deletions of 40 amino acids from the EC3 C-terminus (EC3 –40) led to a loss of signals with mAb 1A5 and a significant decrease in mAb 2C7 binding activity (Fig. 4B). These observations suggest that the mAb 2C7 and 1A5 epitopes recognize amino acids between 343 and 363 (Fig. 4B). EC3 mutants with sequential 5 amino acids deletions between amino acids 333-363 were then generated and the mAb 2C7 and 1A5 epitope was localized to amino acids 343-348 (Fig. 4C). Next, we generated alanine substitution mutants within the sequence YSLKVE corresponding to amino acid 341-348 and confirmed that amino acids 343-348 are critical for the binding of mAb 2C7 (Fig. 4D). Together, these results demonstrate that the mAb 2C7 epitope is localized to amino acids 343-348 within the EC3 domain of Cad11.

mAb 2C7 epitope is involved in Cad11-mediated adhesion

To examine whether the mAb 2C7 epitope is involved in Cad11 adhesion, we generated a Cad11 mutant with alanine substitutions in the YSLKVE sequence corresponding to amino acids 343-348 (Cad11-6A) (Fig. 5A). Previous studies by Patel et al. (8) showed that the tryptophans located at the second and fourth amino acids of the N-terminus of Cad11 were essential for Cad11-mediated adhesion. Indeed, mutation of W2W4 to alanine abolished Cad11's adhesion activity (8, 14). Thus, a Cad11 mutant with alanine substitutions at tryptophan 2 and 4 (Cad11-W2A) was also generated and used as a control (Fig. 5A). Both Cad11-6A and Cad11-W2A mutants were transfected into L-cells. Western blot showed that wild type Cad11 and Cad11-W2A, but not Cad11-6A, were recognized by mAb 2C7 (Fig. 5B). Both cadherin-11 mutants and wild type could be recognized by mAb 5B2H5, which reacts with the cytoplasmic domain. Next, the expression of wild type and Cad11 mutants were examined by immunofluorescence staining. Cell staining with mAb 5B2H5 showed membrane localization of wild type and mutant Cad11 (Fig. 5C). To further examine whether the Cad11 mutants were targeted to the plasma membrane, cells were immunostained for FACS analyses. As shown in Fig. 5D, mAb 2C7 bound to wild-type and Cad11-W2A expressing cells with a mean intensity of 194 and 120, respectively, but much less to Cad11-6A with a mean intensity of 43. Similar differences were observed when the median of intensity was used for comparison (Fig. 5D). The binding of mAb 1A5 to Cad11-6A was also significantly lower than that to wild type Cad11, consistent with the epitope determination. In contrast to mAb 2C7 and 1A5, the binding of mAb 1B9, 1A1, or 4C1 to wild type or Cad11 mutants did not show significant differences (Fig. 5D).

The ability of Cad11-6A to mediate cell aggregation was next examined. Cad11-6A did not show calcium-dependent cell aggregation (Fig. 5E). Cad11-WT and Cad11-W2A were used as positive and negative controls, respectively (8). A cell-to-substrate binding assay was used to further confirm the involvement of the mAb 2C7 epitope in Cad11-mediated adhesion. For these experiments, we employed Cad11-Fc (5) to coat a 96-well plate. While Cad11-WT cells bound to plates coated with Cad11-Fc, Cad11-6A and Cad11-W2A both exhibited binding similar to that observed with control vector-transfected cells (Fig. 5F). These studies identified a novel Cad11 adhesion motif that is necessary for Cad11-mediated adhesion. From these data, we conclude that mAb 2C7 inhibits Cad11-mediated adhesion by binding to a novel adhesion motif within the EC3 domain of Cad11.

mAb 2C7 inhibits the metastasis of PC3-mm2 cells to bone

To examine whether application of mAb 2C7 can inhibit PCa cells metastasize to bone, an experimental metastasis model in which luciferase-labeled tumor cells were injected intracardially into SCID mice was used in our study. Mice were treated with one dose of mAb 2C7 or IgG (1.2 mg/kg, 30 μg/25g mouse), based on the antibody concentration determined from in vitro study (Fig. 3A), through intraperitoneal injection. PC3-mm2-Luc cells were injected into the left ventricle of the mouse heart to disseminate tumor cells via the circulation. Bioluminescent imaging was performed at 3, 8, and 15 days post-injection (Fig. 6A). The luminescence signals from the intracardiac injection of PC3-mm2 cells showed that tumor cells were present not only in the femurs and/or tibias, but also the mandible areas, lymph nodes, and heart. Previous studies by us and several other groups established that the femur and tibia are the major metastasis sites from intracardiac injections of PC3-mm2-Luc cells (2), and hence we focused on these sites of experimental metastasis. Metastasis to other sites such as the mandible area appears to be a rodent-specific event and its relevance to human disease is not clear. In some mice, luminescence was observed in the chest area. This luminescence most likely occurred from leakage of PC3-mm2-Luc cells during injection of cells into the left ventricle. At Day 15, 4 of 5 mice in control group (IgG-treated) developed metastasis in the hind legs (Fig. 6A). In contrast, only one of 5 mice in the mAb 2C7-treated group developed tumors in bone (Fig. 6A) suggesting that mAb 2C7 pre-treatment reduced the incidence of bone metastasis. In the initial experiment, bioluminescence intensity was used to estimate the tumor sizes in each femur/tibia of the control and mAb 2C7-treated mice (Fig. 6A). We found that pre-treatment of mice with mAb 2C7 before tumor inoculation also significantly decreased the tumor burden in bone (Fig. 6B).

Because live animal bioluminescence cannot distinguish whether the tumors are present inside or outside the bones, a second approach was used that involved direct analysis of PC3-mm2-Luc from isolated bone. The muscles from the hind legs were removed to ensure that only the tissue from inside the bone was analyzed. We performed quantitative PCR for human Alu repetitive sequences using total femur/tibia DNA prepared from mouse hind legs harvested at 3-weeks post-injection. Using the PCR approach, we were able to detect signals at the single cell level in the sample, as determined by real-time PCR using a serial dilution of DNA prepared from PC3-mm2 cells. The experiments were repeated two more times and tumor volumes in the hind legs were analyzed by quantitative PCR. Number of tumor cells in bone, calculated based on a standard curve derived from Alu PCR of PC3-mm2 DNA, is shown in Figure 6C. The results show that mAb 2C7 pre-treatment significantly reduced the number of tumor cells in bone. Taken together, these observations demonstrate that blocking Cad11-mediated adhesion is sufficient to reduce PC3-mm2 cells from metastasizing to bone.

DISCUSSION

Patients with advanced PCa are at high risk of developing bone metastasis (1). Development of metastasis in bone has significant impact on the quality of life and survival of the patients (15, 16). Although it is obvious that therapies that prevent bone metastasis would improve the survival and quality of life for men with advanced PCa, no such therapies have been developed so far that prevent PCa bone metastasis in animal models or clinical settings. In this study, we developed two monoclonal antibodies that inhibit Cad11-mediated PCa cell and osteoblast adhesion through binding a 6 amino acid motif in the extracellular domain and showed that inhibition of Cad11-mediated cell-cell adhesion prevents dissemination of the highly malignant PC3-mm2 PCa cells from metastasizing to bone. These findings lay the foundation for developing a Cad11-based antibody therapy that prevents PCa bone metastasis.

Cad11 is a member of the cadherin superfamily. This family of proteins mediates cell-cell adhesion through calcium-dependent homophilic interaction via the 1st extracellular domain (EC1) of the protein (8). From this point of view, antibodies that recognize the homophillic interaction motif should be among the most effective agents that block Cad11 mediated cell-cell adhesions. However, neither of the two most promising antibodies, i.e. mAb 2C7 and 1A5, selected from the 21 monoclonal antibodies against the extracellular domain of Cad11, recognizes the EC1 domain. This observation suggests the possibility that the previously defined homophillic interaction motif in EC1 of Cad11 may not be a good target region for developing therapeutic agents.

In addition to the well-established role of EC1 in cadherin-mediated cell-cell adhesions, there is evidence that additional sites in Cad11 are also involved in mediating homophilic interactions (12). Using atomic force microscopy, Pittet et al. (12) showed that Cad11-mediated adhesion strength is stronger than that in N-cadherin, suggesting that Cad11 may have a unique adhesion mechanism. Pittet et al. (12) further demonstrated that Cad11 bonds are reinforced over time, with two distinct force increments. As a result, several possible models were proposed for the reinforcement of adherens junctions by Cad11. In the proposed adhesion model D (12), it was suggested that a combined strand-dimer as mediated by the EC1, and the EC inter-digitation as mediated through EC1 to EC3, are involved in Cad11-mediated adhesion. Given that both mAb 2C7 and 1A5 recognize the 343-348 region of EC3, we suggest that this EC3 motif is at or within the suspected additional site in Cad11 that cooperates with EC1 in mediating homophilic interactions.

Although direct structural studies are required to define the role of the 343-348 motif of EC3 in the overall homophilic interaction of cell surface Cad11, our finding that both of the selected antibodies recognize this unique adhesion motif supports that this motif is a good target region for developing the second generation of more effective agents for Cad11-based antibody therapy. High affinity antibodies may be developed against this motif plus surrounding regions. In addition, the identification of this motif may also allow the development of peptidomimetic compounds that work similarly as antibodies in blocking Cad11-mediated cell-cell adhesion.

mAb 2C7-mediated decreased metastasis may result from multiple mechanisms. Inhibition of prostate cancer-osteoblast interaction and potentially prostate cell-cell interactions constitutes one of the mechanisms. Because we found that both the size of metastatic lesions in bone and the overall number of metastases are decreased when treated with mAb 2C7 (Figure 6), this observation raises the possibility that other mechanisms may be involved. One possible mechanism is that the antibody therapy may inhibit outgrowth of metastases in bone, in addition to inhibiting PCa targeting to bone. However, our previous studies have demonstrated that knockdown of Cad11 did not have effects on PC-3 tumor growth in bone, based on in vitro proliferation assays (4). Another possibility is that mAb 2C7 may decrease metastasis by promoting cell killing through antibody-mediated mechanisms. Further studies will be required to address these possibilities.

One concern about antibody-based therapy is the potential undesirable toxicity resulting from the involvement of the targeted molecule in normal physiology. Cad11 has been demonstrated to be involved in several developmental processes, including brain development (17-19). In adults, Cad11 is expressed at high levels in osteoblasts and low levels in brain, lung, and testis tissues (13), indicating their continued functions in adult tissues. Importantly, targeted disruption of Cad11 did not affect mouse development except for a small reduction in bone density (20), suggesting that toxicities that might arise from anti-Cad11 therapies are likely to be minimal due to presence of functional redundancy.

Besides preventing bone metastasis, anti-Cad11 antibodies also have potential as therapeutics for rheumatoid arthritis and lung fibrosis. Cad11 is expressed in fibroblast-like synoviocytes (21) and is essential for the development of the synovium (22). In a mouse model, Lee et al. (22) demonstrated that Cad11 is involved in rheumatoid arthritis, which was attenuated by an anti-mouse Cad11 antibody. Schneider et al. (23) showed that Cad11 contributed to pulmonary fibrosis, which could be treated by anti-Cad11-neutralizing monoclonal antibody. Whether these antibodies affect Cad11-mediated adhesion remains to be determined.

PCa cells and osteoblasts also express other cell adhesion molecules such as N-cadherin and integrins. It is likely that these adhesion molecules are also involved in the PCa/osteoblast interactions. Tanaka et al. (24) reported that monoclonal antibodies targeting N-cadherin inhibits PCa cell adhesion to fibronectin and also the migration, invasion, growth, metastasis and castration resistance of PCa. Annexin II and Annexin II receptor axis were also shown to regulate adhesion, migration, homing, and growth of PCa (25). Although mAb 2C7 is able to elicit a significant decrease in bone metastasis in vivo, we predict that strategies targeting additional adhesion molecules or metastasis mediators will further enhance metastasis inhibition.

In summary, we showed that interfering with Cad11-mediated adhesion through a unique adhesion motif at EC3 domain is sufficient for inhibiting the metastasis of PCa to bone. Further development of mAb 2C7 for human use is warranted.

Supplementary Material

Refer to Web version on PubMed Central for supplementary material.

Acknowledgments

This work was supported by National Institutes of Health Grant CA111479, P50-CA140388, CA16647, US Department of Defense Grants PC093132, PC080847, Cancer Prevention and Research Institute of Texas (CPRIT RP110327) and an award from the Prostate Cancer Foundation.

References

1. Tu, S-M.; Lin, S-H. Clinical aspects of bone metastases in prostate cancer. In: Keller, ET.; Chung, LW., editors. The Biology of Bone Metastases. Kluwer Academic Publishers; Boston, MA: 2004. p. 23-46.
2. Chu K, Cheng CJ, Ye X, Lee YC, Zurita AJ, Chen DT, et al. Cadherin-11 promotes the metastasis of prostate cancer cells to bone. Mol Cancer Res. 2008; 6:1259–67. [PubMed: 18708358]
3. Cheng SL, Lecanda F, Davidson MK, Warlow PM, Zhang SF, Zhang L, et al. Human osteoblasts express a repertoire of cadherins, which are critical for BMP-2-induced osteogenic differentiation. J Bone Miner Res. 1998; 13:633–44. [PubMed: 9556063]
4. Huang CF, Lira C, Chu K, Bilen MA, Lee YC, Ye X, et al. Cadherin-11 increases migration and invasion of prostate cancer cells and enhances their interaction with osteoblasts. Cancer Res. 2010; 70:4580–9. [PubMed: 20484040]
5. Lira CB, Chu K, Lee YC, Hu MC, Lin S-H. Expression of the extracellular domain of OB-cadherin as an Fc fusion protein using bicistronic retroviral expression vector. Protein Expr Purif. 2008; 61:220–6. [PubMed: 18620062]
6. Galfione M, Luo W, Kim J, Hawke D, Kobayashi R, Clapp C, et al. Expression and purification of the angiogenesis inhibitor 16 kilodalton prolactin fragment from insect cells. Protein Expr Purif. 2003; 28:252–8. [PubMed: 12699689]
7. Takeichi M. Cadherins: a molecular family important in selective cell-cell adhesion. Annu Rev Biochem. 1990; 59:237–52. [PubMed: 2197976]

8. Patel SD, Ciatto C, Chen CP, Bahna F, Rajebhosale M, Arkus N, et al. Type II cadherin ectodomain structures: implications for classical cadherin specificity. Cell. 2006; 124:1255–68. [PubMed: 16564015]
9. Sivasankar S, Brieher W, Lavrik N, Gumbiner B, Leckband D. Direct molecular force measurements of multiple adhesive interactions between cadherin ectodomains. Proc Natl Acad Sci U S A. 1999; 96:11820–4. [PubMed: 10518534]
10. Chappuis-Flament S, Wong E, Hicks LD, Kay CM, Gumbiner BM. Multiple cadherin extracellular repeats mediate homophilic binding and adhesion. J Cell Biol. 2001; 154:231–43. [PubMed: 11449003]
11. Zhu B, Chappuis-Flament S, Wong E, Jensen IE, Gumbiner BM, Leckband D. Functional analysis of the structural basis of homophilic cadherin adhesion. Biophys J. 2003; 84:4033–42. [PubMed: 12770907]
12. Pittet P, Lee K, Kulik AJ, Meister JJ, Hinz B. Fibrogenic fibroblasts increase intercellular adhesion strength by reinforcing individual OB-cadherin bonds. J Cell Sci. 2008; 121:877–86. [PubMed: 18303045]
13. Okazaki M, Takeshita S, Kawai S, Kikuno R, Tsujimura A, Kudo A, et al. Molecular cloning and characterization of OB-cadherin, a new member of cadherin family expressed in osteoblasts. J Biol Chem. 1994; 269:12092–8. [PubMed: 8163513]
14. Chang SK, Noss EH, Chen M, Gu Z, Townsend K, Grenha R, et al. Cadherin-11 regulates fibroblast inflammation. Proc Natl Acad Sci U S A. 2011; 108:8402–7. [PubMed: 21536877]
15. Jacobs SC. Spread of prostatic cancer to bone. Urology. 1983; 21:337–44. [PubMed: 6340324]
16. Shah RB, Mehra R, Chinnaiyan AM, Shen R, Ghosh D, Zhou M, et al. Androgen-independent prostate cancer is a heterogeneous group of diseases: lessons from a rapid autopsy program. Cancer Res. 2004; 64:9209–16. [PubMed: 15604294]
17. Hadeball B, Borchers A, Wedlich D. Xenopus cadherin-11 (Xcadherin-11) expression requires the Wg/Wnt signal. Mech Dev. 1998; 72:101–13. [PubMed: 9533956]
18. Borchers A, David R, Wedlich D. Xenopus cadherin-11 restrains cranial neural crest migration and influences neural crest specification. Development. 2001; 128:3049–60. [PubMed: 11688555]
19. Backer S, Hidalgo-Sánchez M, Offner N, Portales-Casamar E, Debant A, Fort P, et al. Trio controls the mature organization of neuronal clusters in the hindbrain. J Neurosci. 2007; 27:10323–32. [PubMed: 17898204]
20. Kawaguchi J, Azuma Y, Hoshi K, Kii I, Takeshita S, Ohta T, et al. Targeted disruption of cadherin-11 leads to a reduction in bone density in calvaria and long bone metaphyses. J Bone Miner Res. 2001; 16:1265–71. [PubMed: 11450702]
21. Valencia X, Higgins JM, Kiener HP, Lee DM, Podrebarac TA, Dascher CC, et al. Cadherin-11 provides specific cellular adhesion between fibroblast-like synoviocytes. J Exp Med. 2004; 200:1673–9. [PubMed: 15611293]
22. Lee DM, Kiener HP, Agarwal SK, Noss EH, Watts GF, Chisaka O, et al. Cadherin-11 in synovial lining formation and pathology in arthritis. Science. 2007; 315:1006–10. [PubMed: 17255475]
23. Schneider DJ, Wu M, Le TT, Cho SH, Brenner MB, Blackburn MR, et al. Cadherin-11 contributes to pulmonary fibrosis: potential role in TGF-{beta} production and epithelial to mesenchymal transition. FASEB J. 2011
24. Tanaka H, Kono E, Tran CP, Miyazaki H, Yamashiro J, Shimomura T, et al. Monoclonal antibody targeting of N-cadherin inhibits prostate cancer growth, metastasis and castration resistance. Nat Med. 2010; 16:1414–20. [PubMed: 21057494]
25. Shiozawa Y, Havens AM, Jung Y, Ziegler AM, Pedersen EA, Wang J, et al. Annexin II/annexin II receptor axis regulates adhesion, migration, homing, and growth of prostate cancer. J Cell Biochem. 2008; 105:370–80. [PubMed: 18636554]

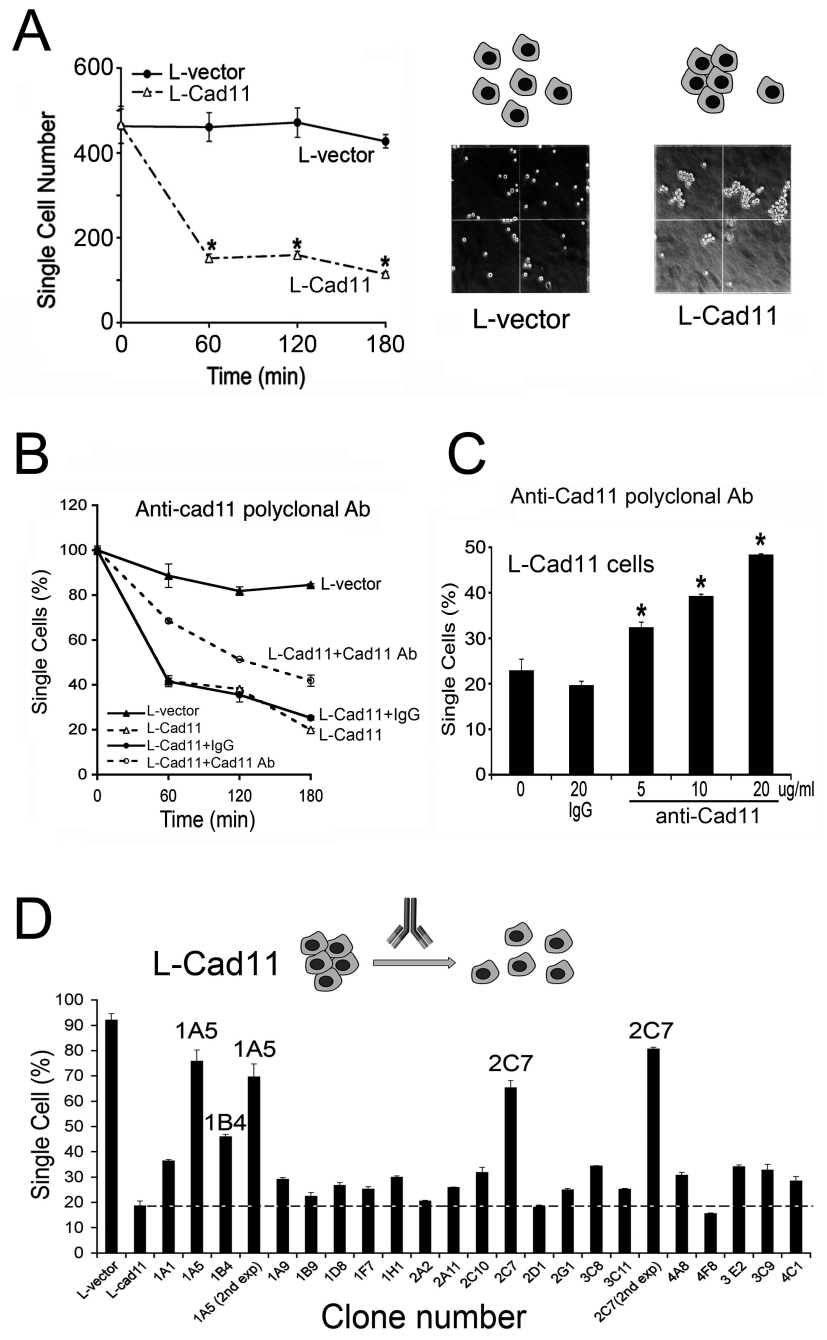

Fig. 1.

L-Cad11 cell aggregation. (A) Time course of Cad11-mediated cell-cell adhesion measured as a decrease in single cell number. L-vector did not exhibit significant aggregation activity. (B) Time course of aggregation inhibition by 20 μg/ml of IgG or anti-Cad11 polyclonal antibody. (C) Dose-dependence of aggregation inhibition by polyclonal anti-Cad11 antibodies. Results from the 3 h assay are shown (*, $p < 0.05$). (D) Screening for adhesion-blocking monoclonal antibodies. L-Cad11 cells were incubated with hybridoma supernatants and the time course of aggregation was measured. Untreated L-vector cells and L-Cad11 cells were used as negative and positive controls, respectively. mAb 1A5 and 2C7 were

assayed twice to confirm that the inhibition was reproducible. Results from the 3 h aggregation assay are shown.

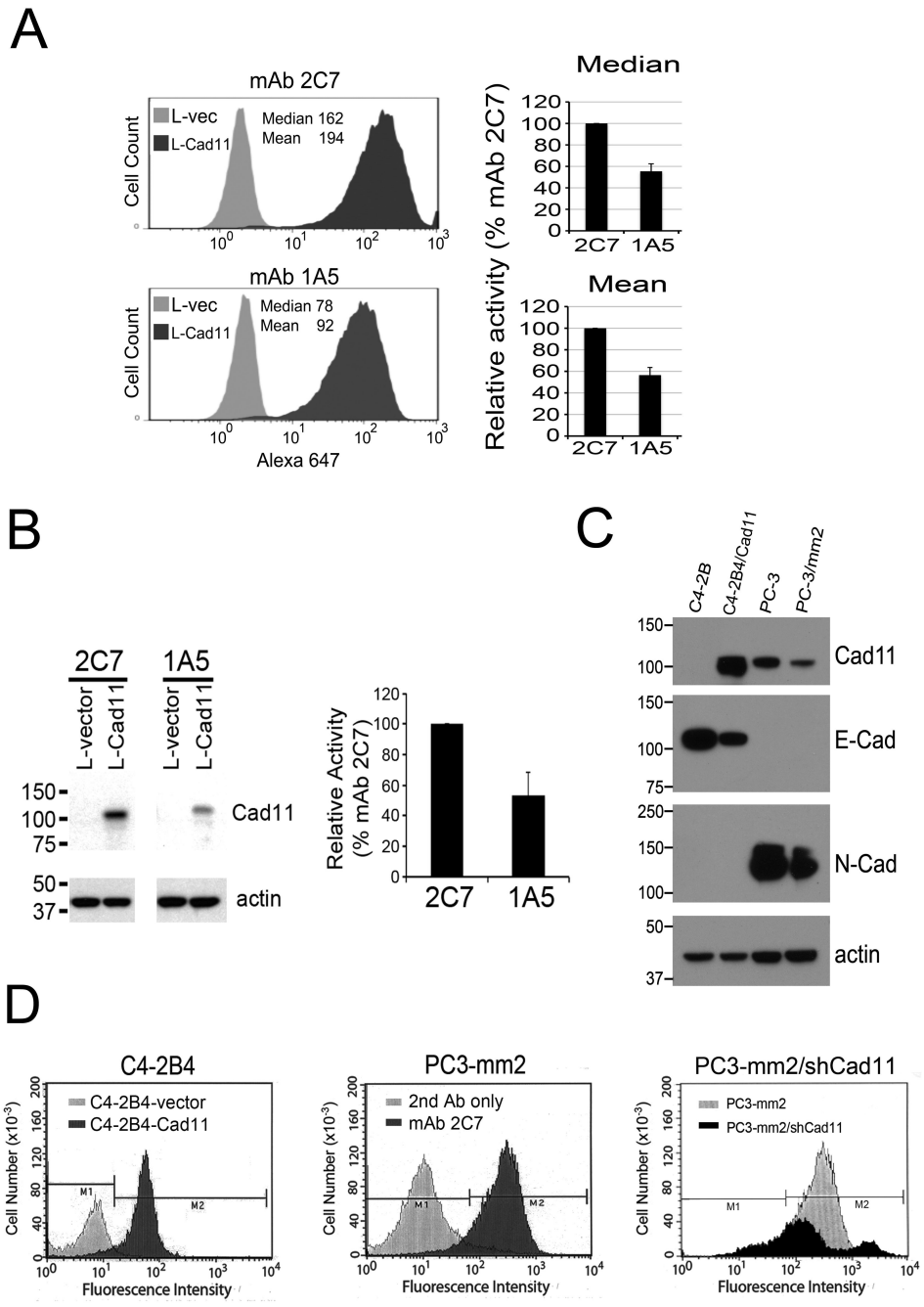

Fig. 2.

Characterization of mAb 2C7 and mAb 1A5 for their affinity and specificity. (A) Fluorescence activated cell sorting (FACS) analysis showed that binding of mAb 2C7 to L-Cad11 cells was two-fold higher than mAb 1A5. (B) Western blotting analysis comparing the activity of mAb 2C7 and 1A5 showed that binding of mAb 2C7 to Cad11 was two-fold higher than mAb 1A5. (C) Western blotting analysis of cell lysates prepared from C4-2B4, C4-2B4/Cad11, PC3, and PC3-mm2 cell lines for the expression of E-cadherin, N-cadherin, and Cad11. mAb 2C7 does not bind to E-cadherin or N-cadherin. (D) FACS of mAb 2C7 with PCa cell lines. 2C7 shows high fluorescence intensity on C4-2B4-Cad11, but not C4-2B4-vector cells. mAb 2C7 shows high fluorescence intensity with PC3-mm2 cells

compared to the cells treated with 2nd antibody only. Knockdown of Cad11 expression by shRNA in PC3-mm2 cells, as described previously (2), significantly decreased the binding of mAb 2C7.

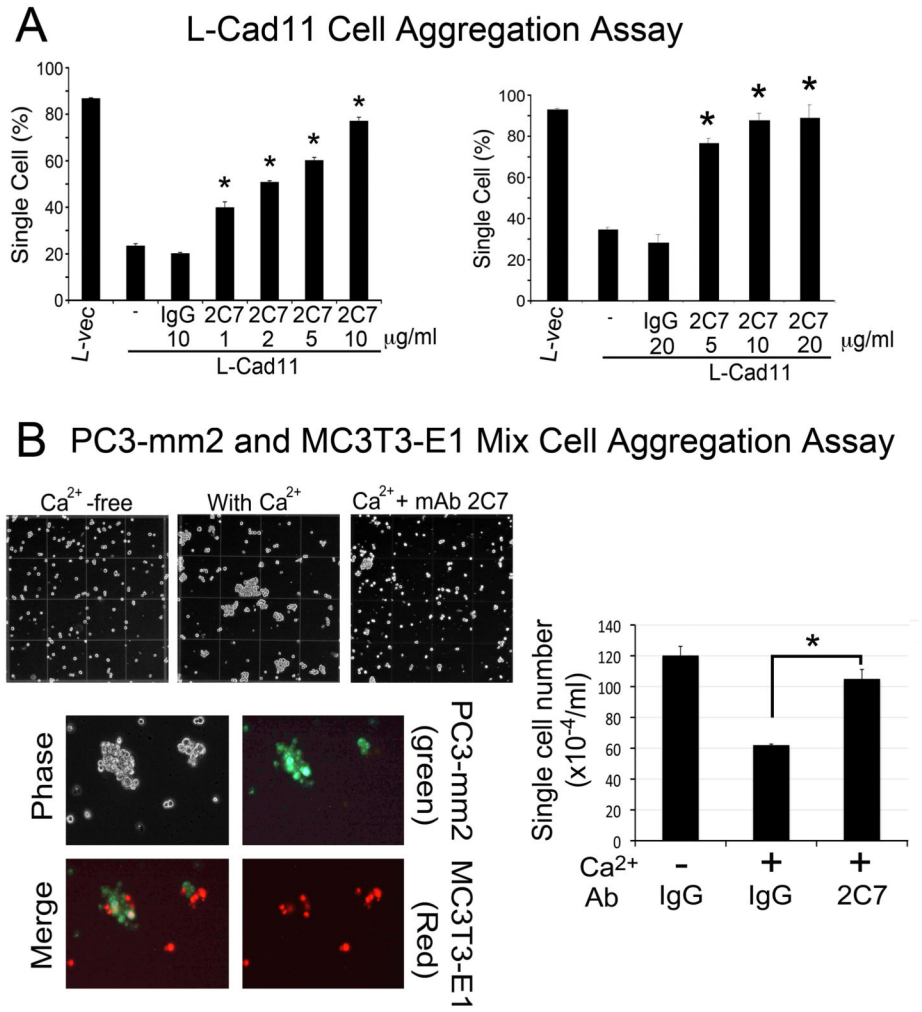

Fig. 3.

mAb 2C7 blocks the aggregation between PC3-mm2 and MC3T3-E1 osteoblasts but not Cad11-mediated migration and invasion. (A) mAb 2C7 showed a dose-dependent inhibition of aggregation with maximal inhibition at 10 μg/ml. Results from the 3 h assay are shown. (B) PC3-mm2 (green) and MC3T3-E1 (red) formed mixed aggregates in the presence of calcium. Addition of mAb 2C7 blocks the Ca^{2+}-induced PC3-mm2/MC3T3-E1 osteoblast aggregation.

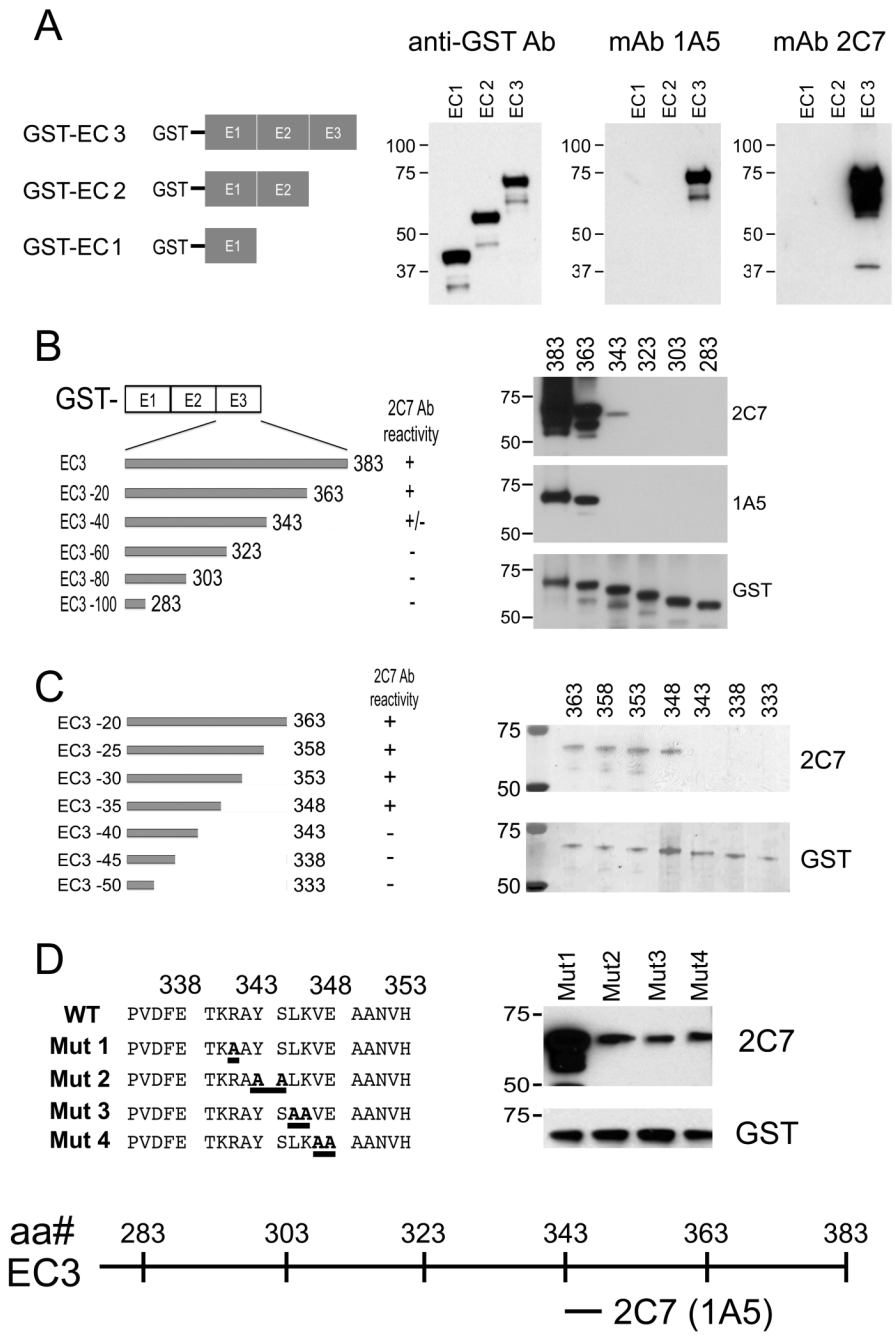

Fig. 4.

Mapping mAb 2C7 and mAb 1A5 epitope in the Cad11 EC3 domain. Western blot of mAb 2C7 and mAb 1A5 with (A) GST-fusion proteins contain 1, 2 or 3 EC domains; (B) Cad11 deletion mutants a series of 20-amino acid deletions from 383 down to 283 amino acids; (C) Cad11 mutants containing a series of 5-amino acid deletions from 363 down to 333 amino acids; (D) Cad11 mutants with alanine substitutions at amino acids 341 to 348. mAb 2C7 and mAb 1A5 bind to the same epitope and is localized at amino acids 343-348 in the EC3 domain.

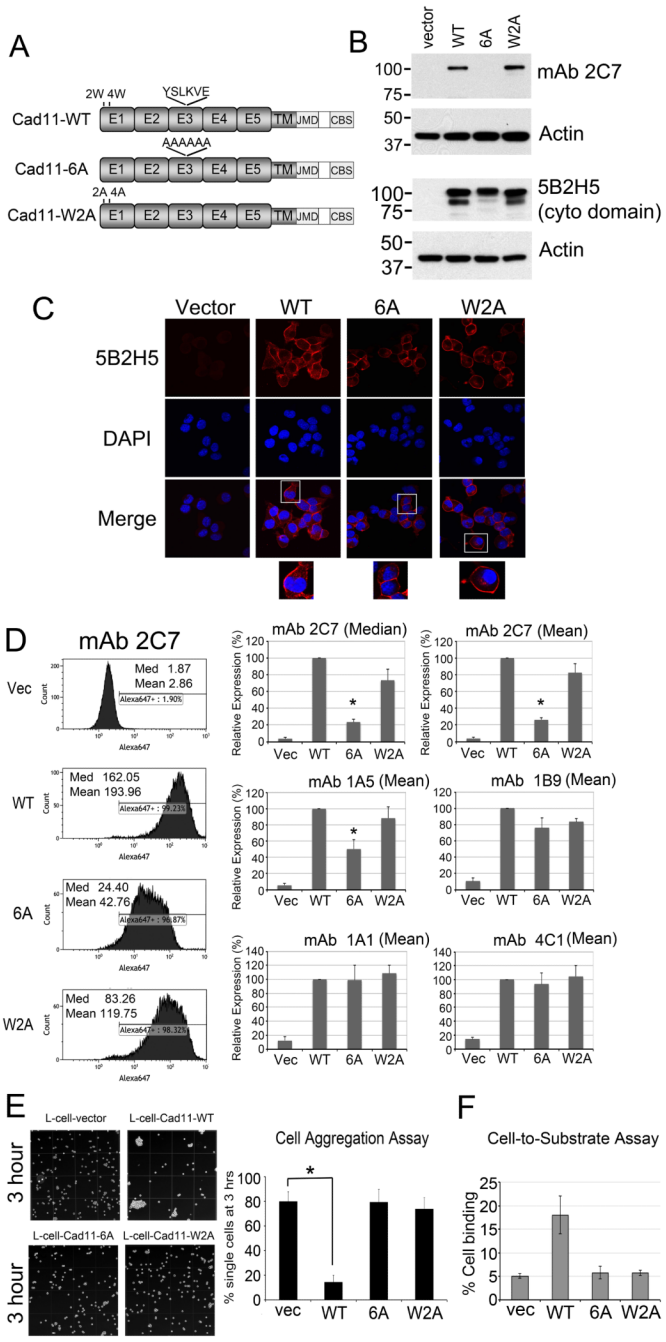

Fig. 5.

Mutation of mAb 2C7 epitope on Cad11 abolished its homophilic adhesion activity. (A) Schematic presentation of Cad11 with mutations of the mAb 2C7 epitope to alanine (Cad11-6A) or mutations of two tryptophans at the N-terminus (Cad11-W2A). (B) Western blot of Cad11 mutants expressed in L-cells. Antibody 5B2H5 that recognizes Cad11 cytoplasmic domain was used as a positive control. (C) Immunofluorescence staining of L-cells expressing Cad11 mutants showed that they are all expressed on the plasma membrane. (D) Characterization of L-cells expressing Cad11 mutants by FACS analysis. Cad11-6A showed decreased binding with mAb 2C7 and mAb 1A5 but not with Cad11 monoclonal antibodies 1B9, 1A1, or 4C1. (E) Cell aggregation assay showed that L-cells expressing

Cad11-WT formed cell aggregation (*, $p < 0.05$) while Cad11-6A and Cad11-W2A could not form cell aggregates. (F) Cell-to-substrate assay showed that only Cad11-WT expressing L-cells were able to bind to a Cad11-Fc-coated dish.

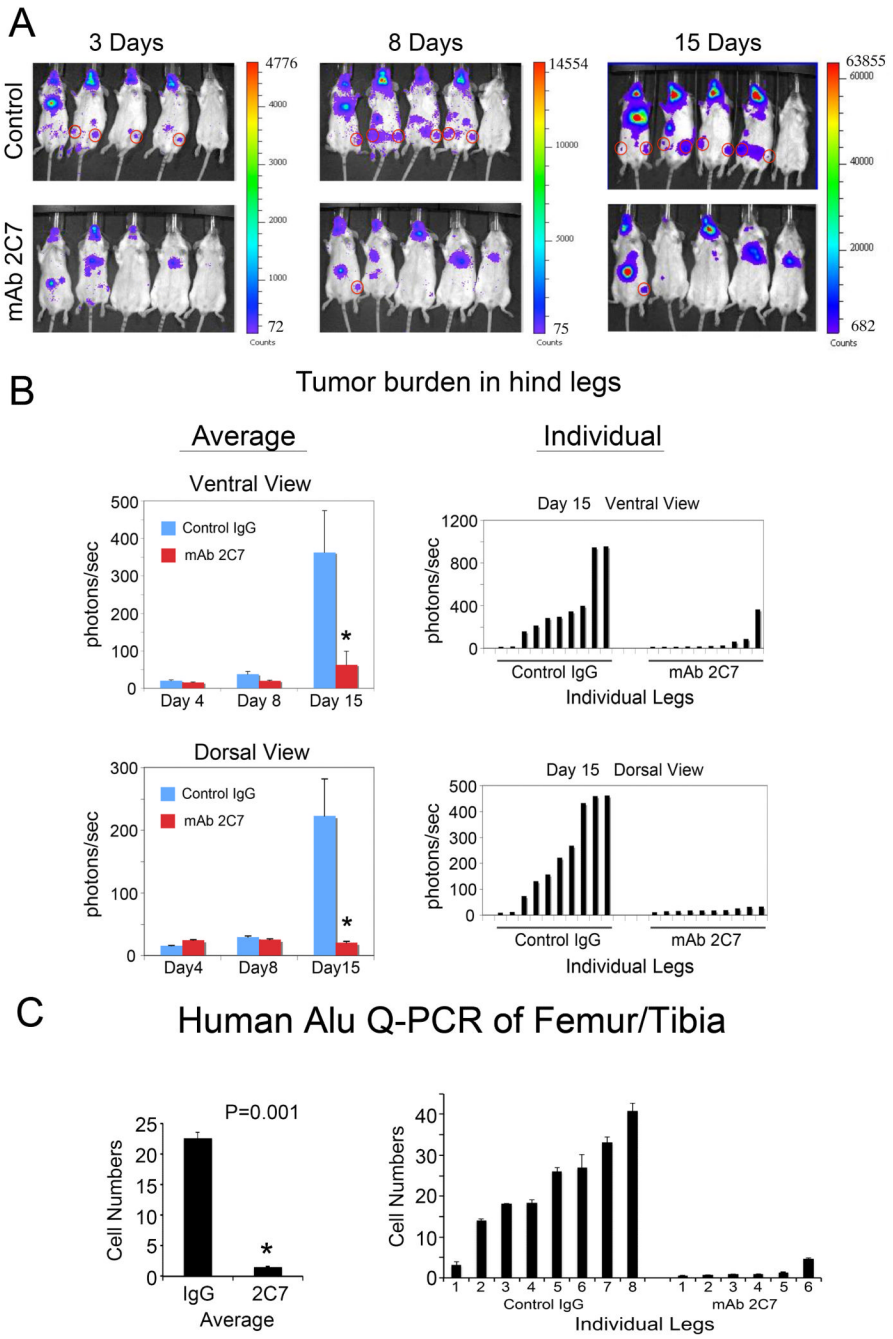

Fig. 6.

mAb 2C7 reduces PC3-mm2 metastasis to bone in a mouse experimental metastasis model. Luciferase-labeled PC3-mm2 cells were injected intracardially into SCID mice. (A) Bioluminescence images of mice. Mice pre-treated with mAb 2C7 formed fewer skeletal metastases (red circles) in hind legs compared to those pre-treated with control IgG. (B) Tumor volume in the hind legs was determined by bioluminescence and expressed as photons per sec. Bioluminescence intensities from both ventral view and dorsal view of mice were determined and used as tumor volume. Left panel, average tumor volume in hind legs. Right panel, tumor volumes in individual hind legs. (C) Tumor volumes in the hind legs were determined by quantitative PCR using primers specific to human Alu sequence.

Five mice were used in the control and mAb 2C7-treated group. Due to one and two mice in the control and treated group, respectively, dying before termination of the study, Alu qPCR was performed on DNAs isolated from femurs/tibias from four mice from the control group and three mice from the treated group. Thus, there are 8 values in control and 6 values in treated mice. 20 ng of total DNA prepared from mouse hind legs was used for PCR. Number of tumor cells in bone, calculated based on a standard curve derived from Alu PCR of PC3-mm2 DNA, is shown.